FLUX DENSITIES IN OPTIMUM NONIMAGING FRESNEL LENS SOLAR CONCENTRATORS FOR SPACE

Ralf LEUTZ, Akio SUZUKI*, Atsushi AKISAWA, Takao KASHIWAGI

Tokyo University of Agriculture and Technology, BASE
2-24-16 Naka-cho, Koganei-shi, Tokyo 184-8588, Japan
phone/fax +81-42-388-7076, email ralfsun@cc.tuat.ac.jp

*UNESCO,
SC/EST, 1, rue Miollis, 75732 Paris Cedex 15, France

ABSTRACT

This paper aims at the clarification of flux density issues in solar Fresnel lens concentrators for use in space photovoltaics. Using the novel nonimaging Fresnel lens designed and prototyped by the authors as example, flux densities are described as dependent on optical concentration ratio of the lens, solar disk size and related brightness distribution, and spectral dispersion of incident sunlight. Discussing the results of a simulation, the optimum linear nonimaging Fresnel lens concentrator is proposed in terms of concentration ratio, i.e. acceptance half angle pairs.

INTRODUCTION

Fresnel lenses have been the concentrators of choice for photovoltaic power generation in space. The use of concentrators tends to minimize both module weight and module cost by substituting cell area with concentrator area; a consequent development is proposed in [1].

Solar concentrators of medium and high concentration ratios require tracking of the sun along one, or two axis. Nonimaging Fresnel lens concentrators can be designed with higher tolerance for tracking errors, accounting for effects due to the size of the solar disk, and unproblematic color behavior, than conventional imaging lenses. One-axis azimuthal tracking is practical for a terrestrial lens module of medium geometrical concentration ratio of approximately 20, translating into acceptance half angle pairs of $\theta = \pm 2°$ and $\psi = \pm 12°$. A schematic of a prototype of the novel nonimaging Fresnel lens is shown in Fig. 1. The design of the novel nonimaging concentrator is described in detail in [2].

FLUX DENSITIES

In [3], Grilikhes has presented a generalized model of sunlight concentration. Differing from this, and bearing in mind the demands of the simulation procedure of the Fresnel lens designed here, the following approach is developed.

The flux density on the absorber can be calculated by tracing incident edge rays from each prism of the lens to the absorber. The edge (outermost) rays for any combination of incidence are traced, and their intersections with the absorber plane are found in a cross-sectional projection, resulting in a part of the absorber plane ΔD being illuminated. The flux density $\delta\xi$ on any part of the absorber plane is found as

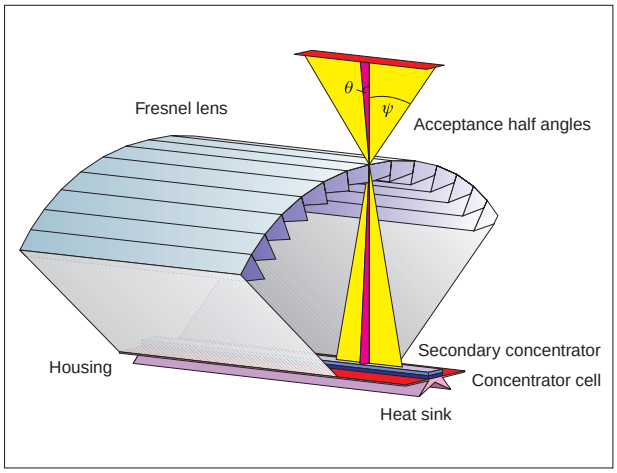

Figure 1: Design study of one-axis tracking terrestrial nonimaging Fresnel lens integrated with photovoltaic concentrator module. Acceptance half angles $\theta = \pm 2°$ in the cross-section (plane of paper), $\psi = \pm 12°$ in the perpendicular plane for a lens with concentration ratio $C = 19.1$. Not to scale.

$$\delta\xi_{\delta d}\left(\theta_{in}, \psi_{in}\right) = \sum_{-i}^{i} w_{e,i}\ \tau_i\ s_i \qquad (1)$$

where the geometrical losses (tip and blocking losses, but not absorber misses) are discounted, resulting in an effective width $w_{e,i}$ of the prism i. Transmittance losses τ accounting for first order reflections are deducted. Depending on the distance of the prism from the absorber, a factor s describing the intensity of the refracted beam on the absorber is calculated

$$s = \Delta D \cos\beta\ l \qquad (2)$$

The prism's height over the absorber plane defines the cosine losses of the beam when hitting the absorber at an angle β other than normal. Closer distance means higher flux density. A factor l is introduced to describe this distance, normalized in respect to the lens height f.

In the simulation, the lens size is individually normalized, as are power densities related to solar disk size with brightness distribution, and power densities attributed to each ray related to spectral irradiance. This results in comparability of lenses of different acceptance half angle pairs, and under different conditions, showing in the shape of the graph of the flux density factor. Thanks to the normalizations, the area under the graph always is unity.

Different acceptance half angles lead to different concentration ratios, or higher flux densities as lenses with higher concentration ratios become wider with constant absorber width, accepting more radiation. To visualize this effect, the flux densities are multiplied with the average concentration ratio of the lens. While this average concentration ratio accounts for reflection losses and geometrical losses at the prisms, it does not consider absorber misses, because these are to be shown in the flux distribution. Thus, resulting flux densities may be exaggerated by a factor estimated at less than 10 percent, depending on the properties of the lens, mainly on the relation ψ/θ.

Solar disk size and brightness distribution

The radius of the solar disk is corresponding to the solar disk half angle, $\theta_s = 0.275°$. This limits the concentration ratio of ideal solar concentrators, which for linear devices is

$$C_{2D,\,max} = \frac{1}{\sin\theta} \approx 208 \qquad (3)$$

The influence of solar disk size on flux density can be simulated by ray tracing. The proper simulation does incorporate the brightness distribution of the solar disk, plotted in Fig. 2, from [4]. The diffusion over the edge of the solar disk is caused by absorption and scattering of radiation in the photosphere of the sun and the atmosphere of the earth.

In the simulation, the brightness distribution is normalized, and a corresponding power density factor attributed to every ray traced trough the prisms of the lens, to the absorber plane. For terrestrial applications, the solar disk and circumsolar radiation are considered, while for the extraterrestrial case, only radiation originating from the solar disk is used to simulate the flux density in the absorber plane of a nonimaging Fresnel lens.

An example showing the insensitivity for solar disk size effects for a lens where the acceptance half angle is larger than the half angle of the sun ($\theta > \theta_s$), is given in Fig. 4 for a lens of acceptance half angle pairs $\theta = \pm 2°$, and $\psi = \pm 12°$. The figure is used also for verification of the simulation, as a prototype exists, where the flux density was measured for the terrestrial case.

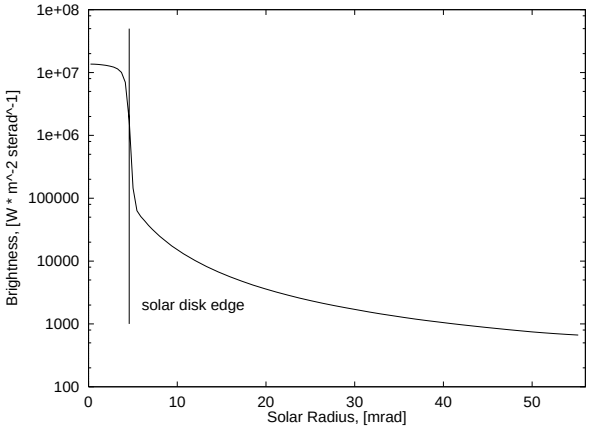

Figure 2: Brightness distribution of the solar disk, using data from [4].

Solar spectral irradiance and color dispersion

Color dispersion leads to aberrations in refractive optical systems, and marks a fundamental difference in the performance evaluation of lenses and mirrors. Nonimaging lens concentrators are relatively insensitive to color dispersion. Radiation of different wavelengths is mixed on the absorber. An indication is the nonexisting rainbow colored edge of the illuminated area on the absorber, that is characteristic to imaging lenses under the sun.

Color behavior, or dispersive power depends on the refractive index n of the lens material, here Polymethylmetacrylate (PMMA) with $n = 1.49$ for yellow light. The refractive index is wavelength dependent, for PMMA over the range of 1.515 to 1.48 from blue to red light.

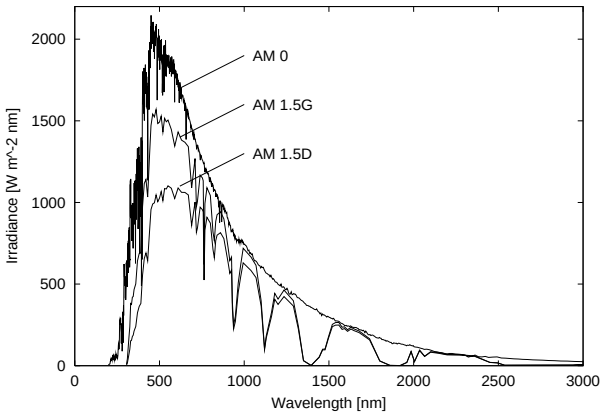

Figure 3: Terrestrial direct-normal (AM 1.5D), terrestrial global-tilt (AM 1.5G), and extraterrestrial (AM 0) standard solar spectral irradiances. Data from [5].

The flux density simulation uses standard solar spectral irradiances ([5], reproduced in Fig. 3) for the extraterrestrial (AM 0) and the terrestrial (AM 1.5D) case to incorporate disperion effects at the rays' refractions.

Each ray thought to be incident on a prism from a point on or near the solar disk carries a normalized power density given by the solar brightness at the point of origin, and one normalized power density decided upon by a color of the respective solar spectrum. All rays of all origins are carrying all colors once; in other words, the solar spectrum is thought to equally originating over the solar disk (and circumsolar radiation). This is an approximation only, for comprehensive data see [6]. Giving an example, [3] describes the radiance of the solar disk to be decreasing towards the edge by 50% in the wavelength range of 450-500 nm, and by 30% in the wavelength range 700-1000 nm.

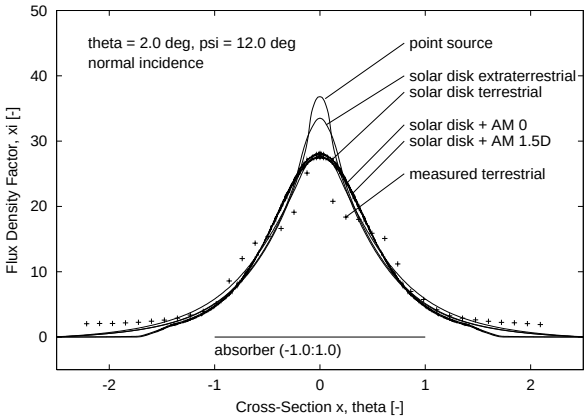

Figure 4: Flux density factors for the nonimaging Fresnel lens of acceptance half angle pairs $\theta = \pm 2°$, and $\psi = \pm 12°$. Measured terrestrial data, comparison with simulated values for point source of radiation, extraterrestrial and terrestrial cases incorporating solar disk size. The effects of the terrestrial direct normal solar spectrum (AM 1.5D) and the extraterrestrial solar spectrum (AM 0) have been added. Normal incidence.

The limits of the solar spectrum for this simulation have been determined by the window of the response range of crystalline Silicone, 300-1200 nm.

The effects of solar disk size and brightness distribution on the one hand, and additional consideration of spectral irradiances on the other hand, have been compared for the terrestrial and extraterrestrial cases in Fig. 4, for a lens of moderate concentration ratio and acceptance half angles much larger than the extension of the solar disk.

Color dispersion changes the resulting flux densities quite significantly, once the acceptance half angle of the concentrator gets close to the radius of the solar disk. The flux densities of a lens of acceptance half angle pairs $\theta = \pm 0.5°$, and $\psi = \pm 3.0°$ have been analysed in the described way. In Fig. 5, flux densities for the cases of point source, solar disk size with extraterrestrial brightness distribution, and solar disk plus dispersion due to the AM 0 spectral irradiance are shown.

The effects shown for normal incidence are similar, and more pronounced for incidence off normal. A modest tracking error of $\theta_{in} = 0.25°$ in the cross-section of

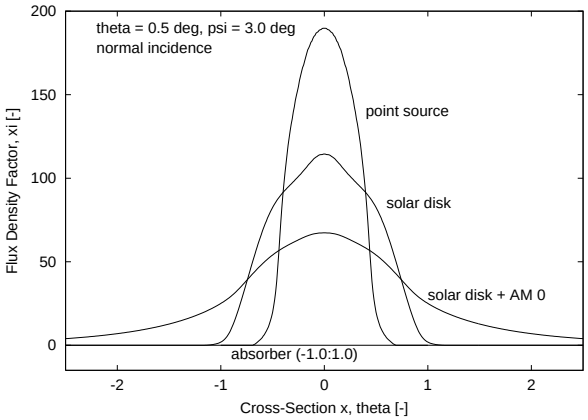

Figure 5: Flux density factors for the nonimaging Fresnel lens of acceptance half angle pairs $\theta = \pm 0.5°$, and $\psi = \pm 3.0°$. Comparison of simulated values for point source of radiation, extraterrestrial solar disk size and brightness distribution, and effects of extraterrestrial solar spectral irradiance on dispersion. Normal incidence.

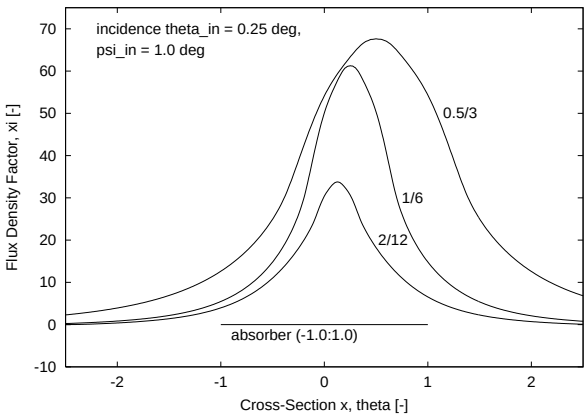

Figure 6: Flux density factors for nonimaging Fresnel lenses. Incidence $\theta_{in} = 0.25°$ in the cross-section of the linear lens (here, from the left in the plane of the paper), and of $\psi_{in} = 1.0°$.

the linear lens, and of $\psi_{in} = 1.0°$ in the perpendicular direction leads to flux densities as shown in Fig. 6. For small acceptance half angles and high concentration ratios, dispersion dominates the flux distribution, setting a practical limit of solar concentration for linear Fresnel lenses (even for nonimaging lenses built from minimum deviation prisms) to about seventy.

For comparison, the flux density distribution on the absorber of a nonimaging Fresnel lens of $\theta = \theta_s = \pm 0.275°$, and $\psi = \psi_s = \pm 0.275°$ is shown for different cases in Fig. 7. This lens represents the highest possible concentration for a linear solar concentrator. Clearly, the concentration is limited by the thermodynamic maximum of Eqn. 3. Once solar disk size and spectral dis-

persion are considered, the flux density of the real lens and the flux density of the nonimaging ideal are very different indeed. Of course, this effect is most pronounced for lenses of high concentration ratios, where the design with yellow light, and the evaluation with white light is least compatible.

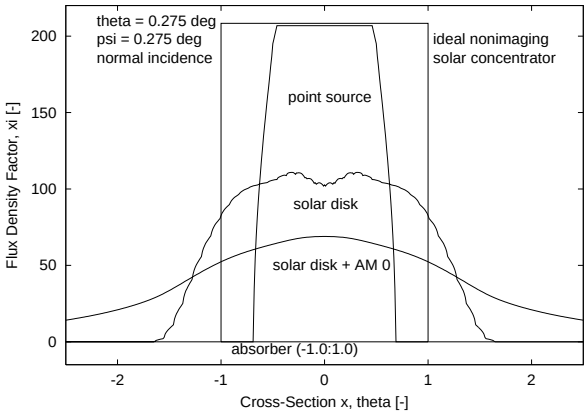

Figure 7: Flux density factors for the nonimaging Fresnel lens of acceptance half angle pairs $\theta = \theta_s = \pm 0.275°$, and $\psi = \psi_s = \pm 0.275°$. Comparison of simulated values for point source of radiation, extraterrestrial solar disk size and brightness distribution, and effects of extraterrestrial solar spectral irradianace on dispersion with flux density distribution of the ideal nonimaging solar 2D-concentrator. Normal incidence.

THE NONIMAGING LENS OF CHOICE

It has been shown that flux density factors in nonimaging Fresnel lens solar concentrators can be strongly influenced by the

- Solar disk size, and to some minor extent brightness distribution over the solar disk and circumsolar radiation (nonparaxial radiation);
- Solar spectral irradiance (color dispersion).

The closer the acceptance half angle to the extension of the solar disk, the greater are the influences of both solar disk size and color dispersion; the latter dominates for lenses of small acceptance half angle pairs, and practically limits the concentration ratio of all lenses. Optimum truncated linear Fresnel lenses may reach a concentration of 70 extraterrestrial suns, roughly one third of the theoretical limit. This ratio is more favourable for lenses of lower concentration.

The differences of the terrestrial case and the extraterrestrial case (different spectra, no circumsolar radiation for the latter) are not very strongly emphasized by the results of a simulation, which uses normalized values of brightness distributions and solar spectral irradiances, and calculates the performance of novel linear nonimaging Fresnel lens concentrators.

Given the technical difficulties related to accurate tracking of the sun, linear concentrators of medium concentration ratio are called for. Losses are progressively increasing for higher concentration ratios. A good choice should be the nonimaging Fresnel lens of acceptance half angle pairs $\theta = \pm 2°$, and $\psi = \pm 12°$. Our lens is easily designed for any tracking accuracy available, and power flux density required; while being relatively insensitive to errors at good optical performance, and showing excellent color behavior.

REFERENCES

[1] M. J. O'Neill, M. F. Piszczor (1997) Inflatable Lenses for Space Photovoltaic Concentrator Arrays; in *Proceedings of the 26th PVSC IEEE Conference*, 30 September-3 October, Anaheim, CA

[2] R. Leutz, A. Suzuki, A. Akisawa, T. Kashiwagi (1999a) Design of a Nonimaging Fresnel Lens for Solar Concentrators; *Solar Energy*, **65**, 6, 379-388

[3] V. A. Grilikhes (1997) Transfer and Distribution of Radiant Energy in Concentration Systems; in: V. M. Andreev, V. A. Grilikhes, V. D. Rumyantsev: *Photovoltaic Conversion of Concentrated Sunlight*, Chichester

[4] A. Rabl (1985) *Active Solar Collectors and Their Applications*; New York

[5] L. D. Partain (ed.)(1995) *Solar Cells and Their Applications*; New York

[6] J. Noring, D. Grether, A. Hunt (1991) Circumsolar Radiation Data: The Lawrence Berkeley Laboratory Reduced Data Base; NREL Report NREL/TP-262-44292; available at *http://rredc.nrel.gov/solar/pubs/circumsolar/*